NO/ NO_x Removal with C_2H_2 as Additive via Dielectric Barrier Discharges

Moo Been Chang and Shyh Chaur Yang
Graduate Institute of Environmental Engineering, National Central University, Chungli, Taiwan 320

Effective reduction and removal of NO_x from gas streams by dielectric barrier discharge (DBD) was studied. A laboratory-scale experimental system was designed and constructed to evaluate the removal efficiency of NO and NO_x. Particularly, C_2H_2 was added as a reducing agent in the $DeNO_x$ plasma process via DBD. Experimental results indicated that the removal efficiency of NO/NO_x increased with increasing applied voltage, gas temperature, and $H_2O_{(g)}$ content. As the oxygen content in the gas stream is increased, more CH_i radicals will be further oxidized to CO_2, thus reducing the removal efficiency of NO_x. When sufficient C_2H_2 was added to the DBD process, as high as 91.2% of NO and 68.2% of NO_x were removed at 140°C for the gas stream containing 500 ppm NO, 1,500 ppm C_2H_2, 3.2% $H_2O_{(g)}$, and 5% O_2, with N_2 as the carrier gas. In addition to N_2 and H_2O, the major products found in this process included NO_2, N_2O, HNO_3, CO_2, CO, and HCOOH, depending on $H_2O_{(g)}$ and O_2 contents of the gas stream.

Introduction

Nitrogen oxides (NO_x) not only lead to the formation of acid deposition and photochemical smog, but also impose adverse effects on human health, vegetation, and materials. As a result, postcombustion $DeNO_x$ processes including the selective catalytic reduction (SCR) and the selective noncatalytic reduction (SNCR) are commonly used for stationary emission control. Nevertheless, these technologies have some unavoidable disadvantages, such as potential poisoning of catalysts and a narrow operational temperature window. Moreover, both technologies can also result in NH_3 slip if not properly handled (Cho, 1994; Chen and Lee, 1996). In order to overcome those disadvantages, developing more effective and environmentally friendly technologies for controlling NO_x emissions has become an important issue. In recent years, development of nonthermal plasmas (NTPs) as an innovative control technology for decomposing noxious pollutants has received much attention. NTPs are noted for creating large number of energetic electrons by the discharge processes. Those electrons can collide with gas molecules in gas streams and then generate highly reactive radicals to react with toxic compounds. NTP technologies have been demonstrated to be effective in removing various gaseous pollutants, for example, SO_x, volatile organic compounds (VOCs), and odor-causing substances from gas streams (Chang et al., 1993; Chang and Lee, 1995; Chang and Tseng, 1996). Therefore, the potential of simultaneous removal of various gaseous pollutants from gas streams may make NTP technologies more appealing than SCR and SNCR.

Various NTP technologies, including electron beam, corona discharge, and dielectric barrier discharge (DBD), have been studied for NO_x removal (Chang et al., 1992; van Veldhuizen et al., 1996; Chang et al., 1996; Chang and Cheng, 1997a). NO_x removal with NTPs can be achieved through two pathways: by chemical oxidation and by chemical reduction. Noticeably, no additive is needed through the pathway of NO_x removal by chemical oxidation. The study conducted by Chang et al. (1992) had investigated the feasibility of directly applying DBD for NO removal by chemical oxidation. More than 95% of NO had been effectively oxidized via highly activated gas-phase radicals (O, OH, and HO_2) to form HNO_3. However, HNO_3 generated through a discharge process will cause a corrosion problem. This concern has greatly limited its applicability in industry. Using corona discharges, van Veldhuizen et al. (1996) pointed out that O_3 also played an important role in oxidizing NO to NO_2 in addition to the oxidative mechanisms proposed by Chang et al. (1992). Their experimental results indicated that the NO conversion was typi-

Correspondence concerning this article should be addressed to M. B. Chang.

cally limited to 60–70% unless very high power was used. Furthermore, they suggested that $DeNO_x$ efficiency could be enhanced if chemicals like H_2O, H_2O_2, O_3, NH_3, or hydrocarbons were introduced into NTPs as an additive. As a result, high efficiency of NO_x removal could be achieved via NTP technologies.

Some additives are necessary for NO_x removal via chemical reduction. In our earlier works, the effects of injecting NH_3 into the $DeNO_x$ plasma process had been experimentally evaluated (Chang and Cheng, 1997a,b). NH_i radicals (including NH_2, NH, and N) generated via NH_3 dissociation with electrons in plasmas can effectively reduce NO to form N_2. Removal efficiency of NO can be further enhanced by raising the gas temperature and by increasing ammonia concentration. Results successfully demonstrate that the $DeNO_x$ plasma process can be performed at room temperature with reasonable removal efficiencies ($\sim 60\%$). Therefore, the disadvantage of a high SNCR operating temperature (900–1100°C) can be overcome. However, the $DeNO_x$ plasma process and traditional SCR/SNCR processes encounter the same problem of NH_3 slip.

Gas reburning has been developed as a $DeNO_x$ technique that utilizes CH_i radicals (such as CH_3, $^1CH_2$, $^3CH_2$, CH, and C) to convert NO_x to N_2 in the presence of O_2. $CH_{i(i=0-2)}$ radicals have been proved effective for NO_x conversion due to their high reactivity with NO (Smyth, 1996). Under fuel-rich conditions, CH_i radicals can chemically reduce NO to nitrogen in the reburning zone of a combustion system (Alzueta et al., 1997). Since the modeling results of Miller and Bowman (1989) indicated that acetylene could be an effective $CH_{i(i=0-2)}$ radical reformer, C_2H_2 is selected as the additive for $DeNO_x$ process via DBD in this study. The major objective of this study is to investigate the effects of operating parameters including applied voltage, gas temperature, O_2, and $H_2O_{(g)}$ contents on the DeNO and $DeNO_x$ removal efficiencies achieved with DBD. Furthermore, byproducts formed in the process are also monitored to gain better insights to this process.

Gas-Phase $DeNO_x$ Mechanisms

This article describes and demonstrates the concept of applying a gas-phase $DeNO_x$ process with C_2H_2 as an additive for generating CH_i radicals (including $^1CH_2$, $^3CH_2$, CH, and C) that can reduce NO_x (including NO and NO_2) to form nitrogen. Formation of CH_i radicals can be achieved via two mechanisms including direct electron dissociation and O radical impacting with C_2H_2 via DBD. Major pathways leading to the reduction of NO_x appear as bold lines in Figure 1 (Thorne et al., 1986; Kline et al., 1989). When CH_i radicals are present in the gas stream, reduction of NO is achieved via Eqs. 1–8. All the rate constants described below are evaluated at 1 atm and 298 K (Smyth, 1996; Miller and Bowman, 1989):

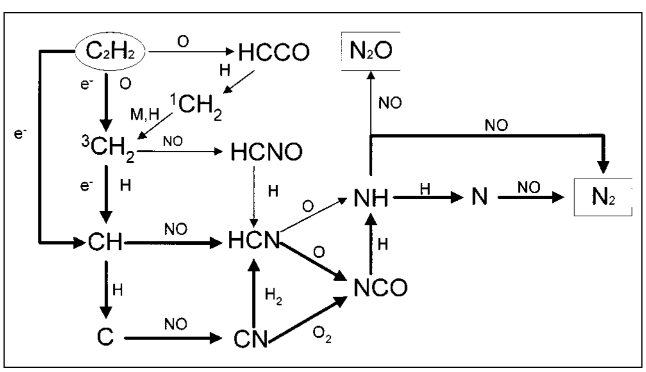

Figure 1. Major pathways leading to NO reduction with C_2H_2 addition.

Reaction Mechanism	k ($cm^3 \cdot s^{-1}$)	
$^3CH_2 + NO \rightarrow HCN + OH$	2.6×10^{-12}	(1)
$^3CH_2 + NO \rightarrow HNCO + H$	2.3×10^{-11}	(2)
$^3CH_2 + NO \rightarrow HCNO + H$	3.1×10^{-12}	(3)
$^1CH_2 + NO \rightarrow HCN + OH$	3.3×10^{-11}	(4)
$CH + NO \rightarrow HCN + O$	8.3×10^{-11}	(5)
$CH + NO \rightarrow NCO + H$	3.3×10^{-11}	(6)
$CH + NO \rightarrow HCO + N$	5.0×10^{-11}	(7)
$C + NO \rightarrow CN + O$	1.1×10^{-10}	(8)

HCN, HCNO, CN, and NCO generated in these reactions are unstable intermediates and can be further converted to N_2 via the reactions with O, H, and N radicals (see Figure 1 and Eqs. 9–12):

Reaction Mechanism	k ($cm^3 \cdot s^{-1}$)	
$HCN + O \rightarrow NCO + H$	1.7×10^{-17}	(9)
$NCO + H \rightarrow NH + CO$	8.3×10^{-11}	(10)
$NH + H \rightarrow N + H_2$	1.7×10^{-10}	(11)
$N + NO \rightarrow N_2 + O$	5.9×10^{-11}	(12)

In addition to the major reductive pathways just described, oxidative $DeNO_x$ reactions cannot be overlooked. Detailed oxidative mechanisms for NO_x removal have been described in various studies and references, for instance, Chang et al. (1992) and Sun et al. (1996). Previous studies have shown that NO_2, N_2O, and HNO_3 can be detected after plasma treatment. In addition to coke, formation of acids containing carbon was also observed when a gas stream containing hydrocarbon additive was processed with pulsed discharge plasmas (Mizuno et al., 1995).

Experimental Setup

Figure 2 illustrates the laboratory-scale experimental apparatus used in this study. It consists of a gas feeding system, a bench-scale DBD reactor, and a gas sampling and detection system. Mass-flow controllers were used to adjust the flow rate of dry-grade feeding gases including N_2, O_2, NO, and C_2H_2. $H_2O_{(g)}$ in the gas stream was controlled by varying the ratio of the humid gas flow rate to the dry gas flow rate and was measured with a dew point hygrometer (General Eastern Instruments, Model M2). The coaxial wire-tube DBD reactor was made with a crystal-quartz tube with an inner diameter of 4 cm and a length of 69 cm. The inner electrode was made

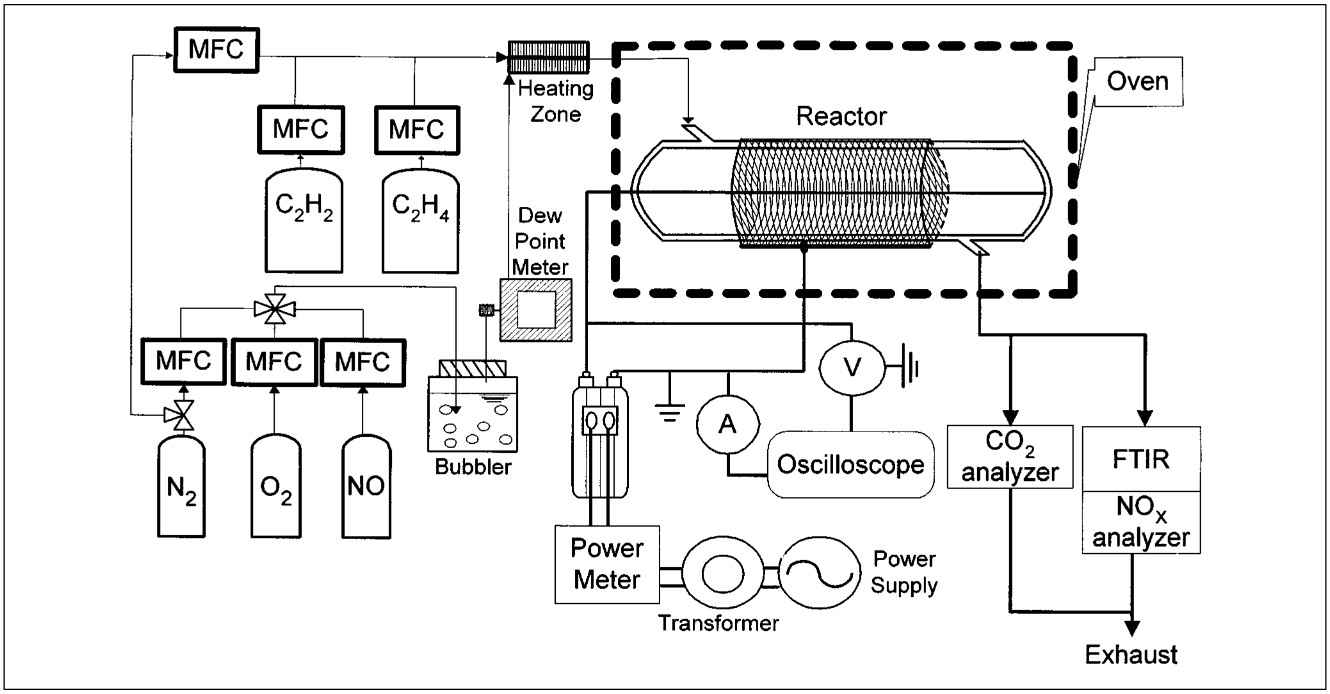

Figure 2. Experimental setup.

of a tungsten rod with a diameter of 2.5 mm. The discharge volume was about 237.4 cm^3, which was sustained by a variable alternating-current voltage transformer operating at 60 Hz.

A Fourier transform infrared (FTIR) spectrometer (Bio-Rad, Model FTS 165), an NO_x analyzer (Rotork, Model 443), and a CO_2 analyzer (Signal, Model 2200) were connected on-line to identify and measure the final products. A FTIR spectrometer was used to detect the byproducts, including C_2H_2, CO, CO_2, HCOOH, NO, NO_2, HCN, and HNO_3. Nonetheless, the characteristic signals of interested compounds may overlap one another, and make it difficult to quantify all kinds of products via FTIR. Therefore, other apparatuses like NO_x analyzer and CO_2 analyzer were used to determine the concentration of NO, NO_2, and CO_2 in the gas stream. HCN was measured by collecting the gas sample with the basic aqueous solution and analyzed using the colorimetric method (Clesceri et al., 1989).

The effect of C_2H_2 concentration on the NO/NO_x removal had been tested prior to the experimental works. Four concentrations of C_2H_2 (500, 1,000, 1,500, and 2000 ppmv) had been chosen to address this issue. Experimental results show that the NO removal increases with increasing acetylene content, and the increasing trend becomes saturated as the C_2H_2 content is further increased from 1,500 ppmv to 2,000 ppmv. For better use of the additive, the C_2H_2 content was then kept at 1,500 ppmv throughout the study.

Typically, the inlet gas streams contain 500 ppmv NO and 1,500 ppmv C_2H_2. Experiments were conducted at room temperature ($\sim$ 25°C) and atmospheric pressure unless specified. In order to reach complete mixing before applying power to the DBD reactor, the gas stream was generated with known composition and inlet gas flow rate and passed through the reactor for 5 min at least. Initial conditions for each test were recorded when the system reached steady state. Total gas flow rates were balanced at 1 slpm with N_2 as the carrier gas for all experiments. Then, the applied voltage was increased in a stepwise manner to values between 12 and 20 kV (rms value) to generate plasmas. Removal efficiency of NO_x (η_{NO_x}) was then calculated as

$$\eta_{NO_x}(\%) = \frac{[NO_x]_{off} - [NO_x]_{on}}{[NO_x]_{off}} \times 100\%. \tag{13}$$

The subscripts in Eq. 13 denote whether the power supplied to the DBD reactor was turned on or shut off. A similar equation and denotation were used to calculate the efficiencies of NO removal (η_{NO}) and C_2H_2 decomposition ($\eta_{C_2H_2}$).

Results and Discussion

Dependence of η_{NO} and η_{NO_x} on applied voltage at various inlet $[O_2]$ (O_2 concentration) is shown in Figure 3. The gas stream contains 500 ppm NO and 1,500 ppm C_2H_2, with N_2 as the carrier gas. The gas flow rate and temperature are controlled at 1 slpm and 25°C, respectively. In the absence of O_2, most of NO_x can be effectively reduced by $CH_{i(i=0-2)}$ and N radicals. With O or O_2 existing in gas streams, however, it will be difficult to directly convert NO_x to N_2. Therefore, the effect of O_2 content must be taken into account. The η_{NO} increases as the inlet $[O_2]$ increases, due to the generation of more oxidative species, including O^-, O, O_2, and O_3. These dominant oxidative radicals in this process result in NO oxidation and NO_2 formation. On the other hand, the η_{NO_x} decreases with the increasing O_2 content, since reductive radicals like $CH_{i(i=0-2)}$ can be oxidized to CO and CO_2 more easily as more O_2 is added to the gas stream (Alzueta et al., 1997; Volponi and Branch, 1992). Consequently,

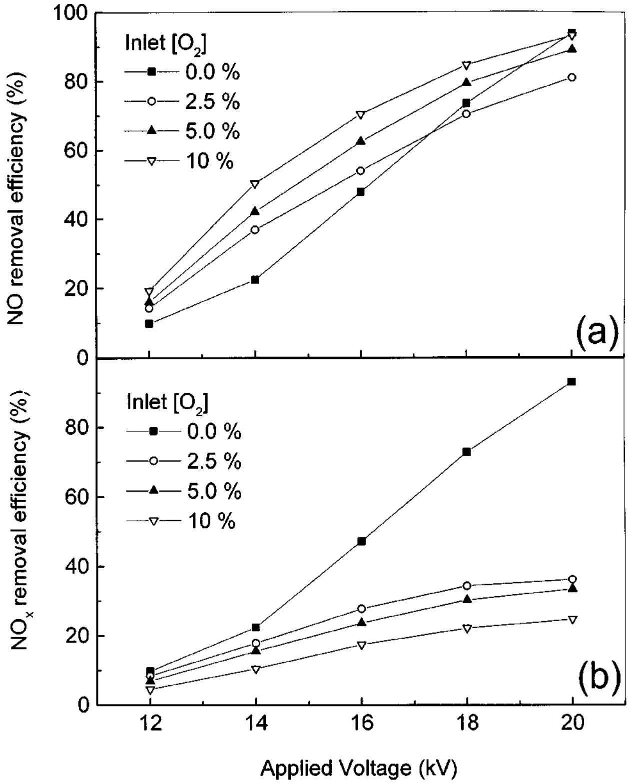

Figure 3. Dependence of (a) NO and (b) NO_x removal efficiency on applied voltage for inlet O_2.

It varied from 0 to 10% by volume ([NO] = 500 ppm, [C_2H_2] = 1,500 ppm, $Q = 1$ slpm, $T = 25°C$).

increasing the inlet [O_2] will increase η_{NO} but decrease η_{NO_x} in the DeNO_x plasma process with C_2H_2 as an additive.

The dependence of $\eta_{C_2H_2}$ on the applied voltage at varying inlet [O_2] is shown in Figure 4. Theoretically, when O_2 is introduced into the system, the most important reaction for consuming C_2H_2 is via its reaction with O to generate CH_2 and CH radicals (Volponi and Branch, 1992). As the $\eta_{C_2H_2}$ is increased, more $CH_{i(i=0-2)}$ radicals should be generated for higher NO_x removal (see Figure 4). Experimental results indicate that the $\eta_{(C_2H_2)}$ increases with increasing [O_2] for the gas stream containing 500 ppmv of NO. As the inlet [O_2] is increased, however, $\eta_{(NO_x)}$ achieved with this process actually decreases (see Figure 3b). The apparent contradiction is caused by the oxidation of $CH_{i(i=0-2)}$ with O atoms to form CO and CO_2 at high inlet [O_2]. The η_{NO_x} cannot be enhanced due to the depletion of $CH_{i(i=0-2)}$ radicals and generation of $CO_{x(x=1-2)}$, which are ineffective for NO_x reduction. Dependence of CO_2 and CO formation on the applied voltage for varying O_2 content is shown in Figure 5. As inlet [O_2] is increased, more CH_i radicals and CO can be oxidized to form CO_2, resulting in the increase of [CO_2]. With the higher applied voltage (18 or 20 kV) and 10% of oxygen content, most CO produced in the DBD system was actually converted to CO_2. Higher production of [CO_2] mainly resulted from CO and $^3CH_2$ oxidative reactions (that is, $CO + O + M \rightarrow CO_2 + M$, $CO + OH \rightarrow CO_2 + H$, $^3CH_2 + O_2 \rightarrow CO_2 + H_2$, and $NO_2 + CO \rightarrow NO + CO_2$).

The effect of the operating temperature on the η_{NO} and η_{NO_x} is shown in Figure 6 for the gas streams containing 5% O_2 by volume. Gas temperature can affect NO/NO_x removal efficiency in three aspects, that is, *E/N*, rate constant, and gas residence time. *E/N* is an important factor affecting the occurrence and performance of gas discharge, while the rate constant governs the chemical kinetic in gas-phase reactions. The decrease of gas residence time caused by the increase of gas temperature would decrease the NO/NO_x removal; however, the extent is negligible compared to the effects of *E/N* and rate constant. At constant gas flow rate and operating temperature, increasing applied voltage tends to increase *E/N*, which would affect the electron energy distribution. Increasing *E/N* can supply electrons with higher energy in the DBD system. When the applied voltage is increased, *E* increases and plasma reactions can be further enhanced. Likewise, if the operating temperature is increased while gas

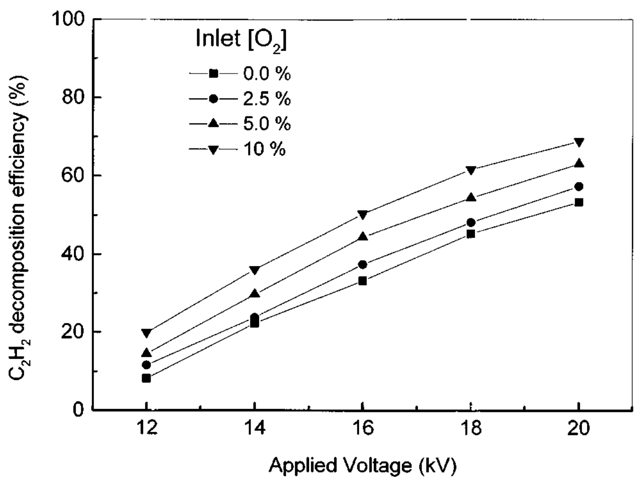

Figure 4. Dependence of C_2H_2 decomposition efficiency on applied voltage for inlet O_2.

It varied from 0 to 10% by volume ([NO] = 500 ppm, [C_2H_2] = 1,500 ppm, $Q = 1$ slpm, $T = 25°C$).

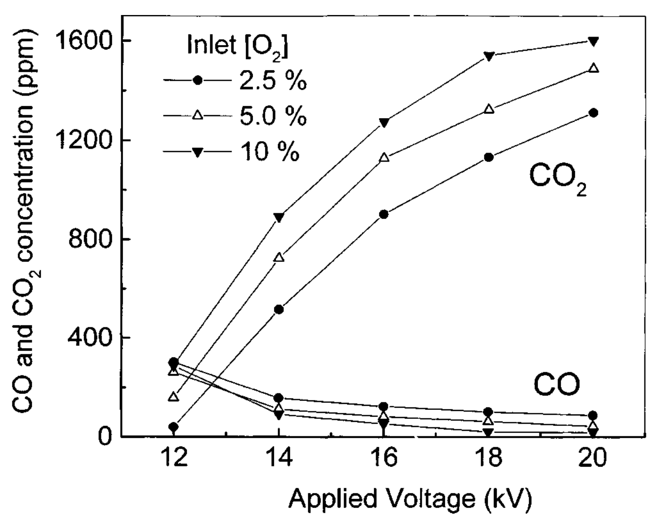

Figure 5. Dependence of CO_2 and CO formation on applied voltage for inlet O_2.

It varied from 0 to 10% by volume ([NO] = 500 ppm, [C_2H_2] = 1,500 ppm, $Q = 1$ slpm, $T = 25°C$).

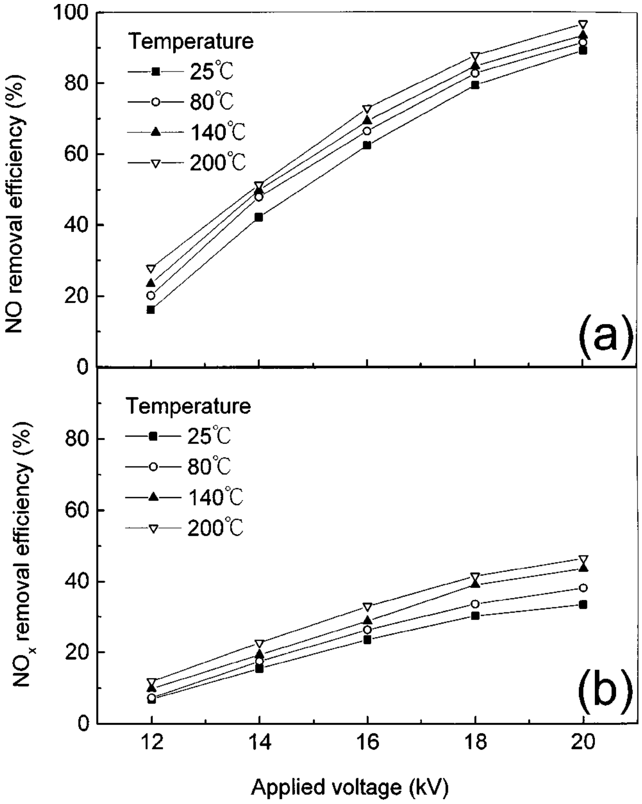

Figure 6. Dependence of (a) NO and (b) NO_x removal efficiency on applied voltage for different operating temperatures.

([NO = 500 ppm, $[C_2H_2] = 1{,}500$ ppm, $[O_2] = 5\%$, $Q = 1$ slpm).

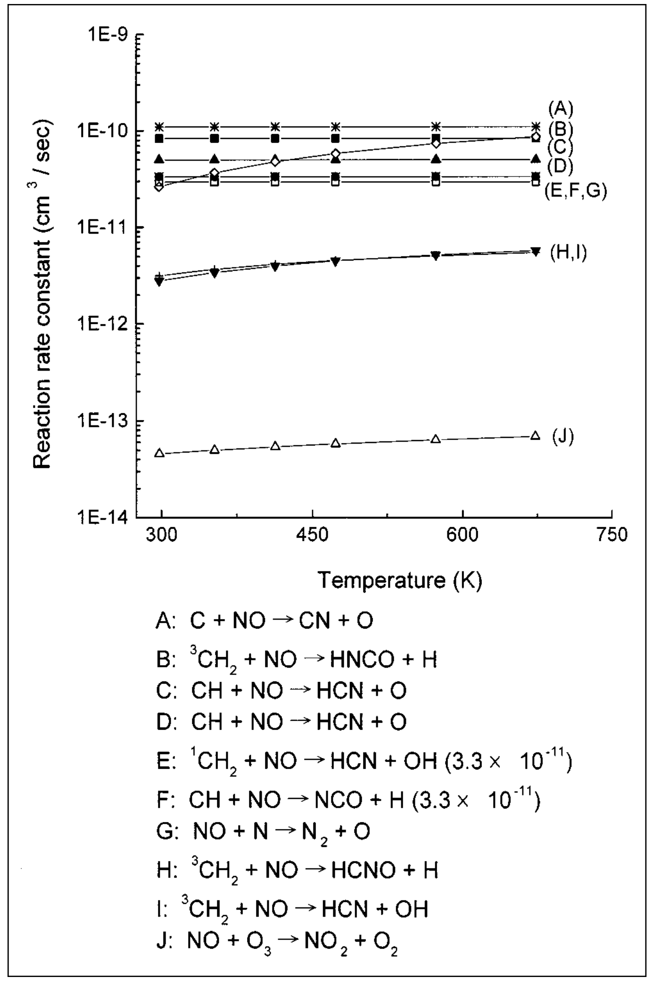

Figure 7. Dependence of major $DeNO_x$ reaction-rate constants on selected temperature.

(Range: $1.0 \times 10^{-14} \sim 1.0 \times 10^{-9}$).

pressure and applied voltage are kept constant, N decreases and then E/N increases. At the same temperature, operating at a higher applied voltage would enhance η_{NO} and η_{NO_x} due to the increased E/N. In addition, as the operating temperature is increased, η_{NO} and η_{NO_x} both increase as well. For a reaction temperature of 200°C, η_{NO} reaches 96.5% while η_{NO_x} is only 46.3%. In other words, about half of the reacted NO was actually oxidized to form NO_2.

As stated previously, a higher operating temperature in the DBD system can enhance $DeNO_x$ efficiencies in general. Figure 7 show the dependence of major $DeNO_x$ reaction rate constants on the gas temperature. Among those reactions shown in Figure 7, most reaction rate constants do not significantly change with the temperature of interest in this study except for the reactions involving with $^3CH_2$ and O_3. Since less O_3 is formed as the gas temperature is increased, the effect of O_3 becomes less important with increasing temperature. When the operating temperature is increased gradually, higher η_{NO} and η_{NO_x} can be achieved mainly due to the accelerated reactions of $^3CH_2 + NO$. Furthermore, the dependence of C_2H_2 decomposition rate on the temperatures is shown in Figure 8. As the operating temperature is increased, the C_2H_2 decomposition rate increases as well, resulting in more $CH_{i(i=2-0)}$ with constant inlet $[O_2]$.

The dependence of η_{NO} and η_{NO_x} on applied voltage for gas streams containing water vapor ranging from 1,100 ppmv

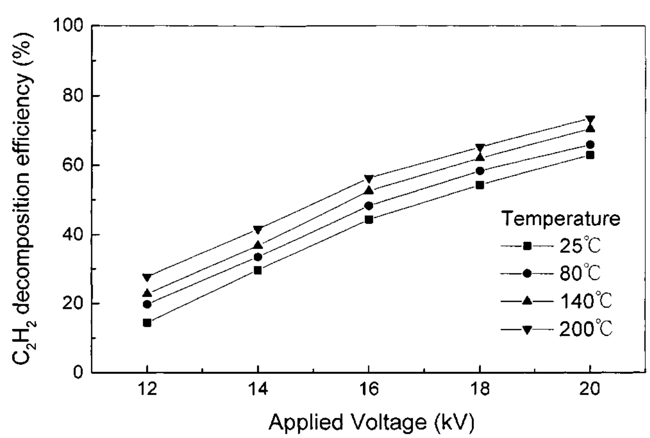

Figure 8. Dependence of C_2H_2 decomposition efficiency on applied voltage for different operational temperature.

($[NO] = 500$ ppm, $[C_2H_2] = 1{,}500$ ppm, $[O_2] = 5\%$, $Q = 1$ slpm).

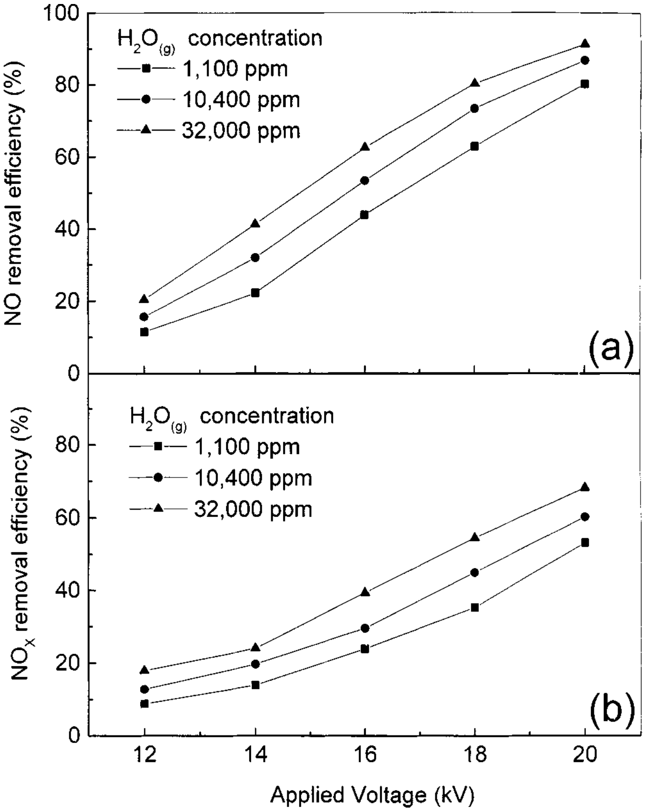

Figure 9. Dependence of (a) NO and (b) NO_x removal efficiency on applied voltage for different inlet $H_2O_{(g)}$ concentrations.

([NO] = 500 ppm, [C_2H_2] = 1,500 ppm, [O_2] = 5%, T = 140°C, Q = 1 slpm).

to 3.2% by volume is shown in Figure 9. The temperature and inlet [O_2] of the gas streams were controlled at 140°C and 5% by volume, respectively. As [$H_2O_{(g)}$] is increased, more OH and HO_2 radicals can be generated to oxide NO to form NO_2 and further to HNO_3 (that is, $NO_2 + OH \rightarrow HNO_3$ and $NO + HO_2 \rightarrow NO_2 + OH$). Therefore, η_{NO} and η_{NO_x} both increase with the increasing $H_2O_{(g)}$ concentration. Experimental results indicate that as high as 91.2% of NO and 68.2% of NO_x are removed at 140°C for the gas stream containing [NO]/[C_2H_2]/[$H_2O_{(g)}$]/[O_2] = 500 ppm: 1,500 ppm: 3.2%: 5%, with N_2 as the carrier gas.

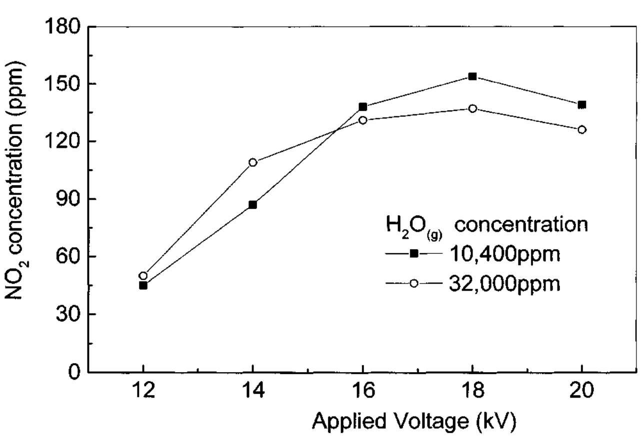

Figure 10. Dependence of NO_2 concentration on applied voltage for different inlet $H_2O_{(g)}$ concentrations.

([NO] = 500 ppm, [C_2H_2] = 1,500 ppm, [O_2] = 5%, T = 140°C, Q = 1 slpm).

Figure 10 shows the dependence of [NO_2] on applied voltage for an inlet [$H_2O_{(g)}$] of 1.04% and 3.2%. As the applied voltage is increased from 12 kV to 18 kV, [NO_2] increases and then reaches the maximum value. As the applied voltage is further increased from 18 kV to 20 kV, part of NO_2 could be further oxidized to form HNO_3 (that is, $NO_2 + OH \rightarrow HNO_3$), resulting in a higher η_{NO_x}, as shown in Figure 9b. This observation implies that operating at a high voltage can lead to more OH and HO_2 radicals, which are responsible for removing NO and NO_2 in the DBD system. It is also clear that higher inlet [$H_2O_{(g)}$] can further decrease [NO_2], and hence increase η_{NO_x}. As the inlet [$H_2O_{(g)}$] is increased from 1.04% to 3.20%, [NO_2] decreases from 139 ppm to 119 ppm at an applied voltage of 20 kV. In this study, HNO_3 is detected only for the gas stream containing [$H_2O_{(g)}$] that is processed with DBDs.

Typical FTIR adsorption spectra before the DBD plasma process without or with 3% [$H_2O_{(g)}$] are shown in Figure 11a and Figure 12a, respectively. The adsorption spectra after the

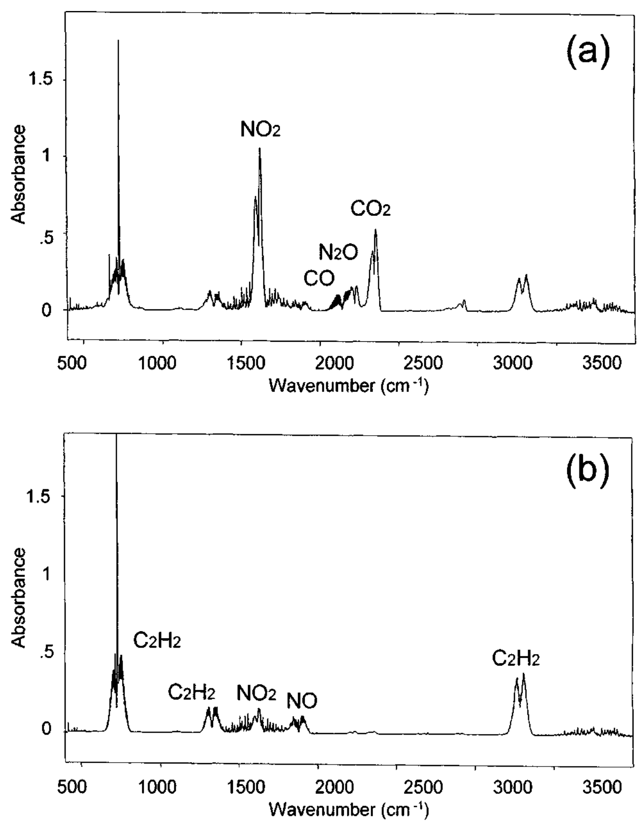

Figure 11. FTIR absorption spectra of the gas mixture before (a) and after (b) $DeNO_x$ plasma treatment with C_2H_2 addition.

Initial conditions: [C_2H_2] = 1,500 ppm, [O_2] = 5%, T = 140°C, Q = 1 slpm.

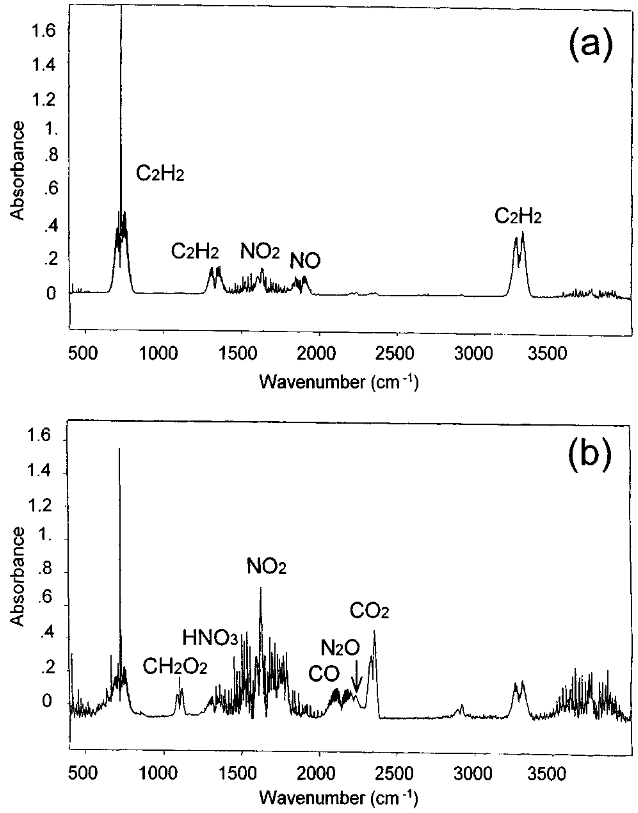

Figure 12. FTIR absorption spectra of the gas mixture (a) before and (b) after DeNO$_x$ plasma treatment with C_2H_2 addition.

Initial conditions: $[C_2H_2] = 1{,}500$ ppm, $[NO] = 500$ ppm, $[O_2] = 5\%$, $[H_2O_{(g)}] = 3\%$, $T = 140°C$, $Q = 1$ slpm.

DBD plasma process for gas streams without and with water vapor at the applied voltage of 20 kV are shown in Figure 11b and Figure 12b, respectively. Except for the minor products of HCOOH and HNO_3, concentrations of most byproducts were quantitatively evaluated. Spectra presented in Figure 11a and Figure 12a show that even without plasma generation, NO can be partially oxidized to NO_2 (< 45 ppm) if the gas stream contains O_2. However, at least 90% of the inlet NO_x remains as NO for all experiments in this study.

From Figure 11b it can be seen that major products include NO_2, N_2O, CO, and CO_2 for the gas stream containing no water vapor. The HCN spectrum, whose characteristic wave numbers are located between 712.3 and 712.7 cm^{-1}, is overlapped by the spectra of C_2H_2 and cannot be accurately measured by FTIR. Therefore, a colorimetric method was used to quantify it, and about 16 ppm of HCN was detected in the exhaust gas. As far as the carbon balance value is concerned, it decreases from 0.94 to 0.79 as the applied voltage was increased from 12 kV to 20 kV. The decrease of the carbon balance value with increasing applied voltage is attributed to the generation of more unknown particulate matters and coke, which are deposited on the inner wall of reactor.

As shown in Figure 12b, FTIR spectra show that major products include NO_2, N_2O, HNO_3, CO_2, CO, and HCOOH for the gas streams containing 3% $H_2O_{(g)}$. Comparing Figure 11b with Figure 12b, we observe that NO_2 apparently decreases, for some NO_2 is converted to form HNO_3, with 3% $[H_2O_{(g)}]$ existing in the gas stream. In addition, 11 ppm of HCN was found in this part of the experiment. Experimental results also indicated that the carbon balance value decreased from 0.95 to 0.77 as the applied voltage was increased from 12 kV to 20 kV.

Conclusions and Recommendations

The effectiveness of applying DBD with C_2H_2 as an additive to generate $CH_{i(i=0-2)}$ radicals for NO_x removal was experimentally evaluated with a laboratory-scale apparatus. Experimental results have demonstrated that both η_{NO} and η_{NO_x} can be enhanced with increasing applied voltage and/or gas temperature. Increasing oxygen content causes $CH_{i(i=0-2)}$ radicals to be oxidized to form CO_2 more easily, which may result in the reduction of η_{NO_x}. $H_2O_{(g)}$ in the gas streams has a distinct influence on NO_x removal. Increasing the inlet $[H_2O_{(g)}]$ can effectively convert NO_2 to form HNO_3 in the DBD system, so η_{NO_x} can be further enhanced. In addition to N_2 and H_2O, final products including NO_2, N_2O, HNO_3, HCN, CO_2, CO, and HCOOH were detected, depending on the inlet $[H_2O_{(g)}]$. In brief, this study has demonstrated that the DBD system with C_2H_2 as an additive is effective for NO_x removal. Further studies on a more accurate measurement of power consumption should be carried out for practical application in industry.

Literature Cited

Alzueta, M. U., P. Glarborg, and K. D. Johansen, "Low Temperature Interactions Between Hydrocarbons and Nitric Oxide: An Experimental Study," *Combust. Flame*, **109**, 25 (1997).

Chang, J. S., P. C. Looy, K. Nagai, T. Yoshioka, S. Aoki, and A. Maezawa, "Preliminary Pilot Tests of a Corona Discharge-Electron Beam Hybrid Combustion Flue Gas Cleaning System," *IEEE Trans. Ind. Appl.*, **32**, 131 (1996).

Chang, M. B., M. J. Kushner, and M. J. Rood, "Gas Phase Removal of NO from Gas Streams via Dielectric Barrier Discharges," *Environ. Sci. Technol.*, **26**, 777 (1992).

Chang, M. B., M. J. Kushner, and M. J. Rood, "Removal of SO_2 and NO from Gas Streams via Combined Plasma Photolysis," *J. Environ. Eng., ASCE*, **119**, 414 (1993).

Chang, M. B., and C. C. Lee, "Destruction of Formaldehyde with Dielectric Barrier Discharge Plasmas," *Environ. Sci. Technol.*, **29**, 181 (1995).

Chang, M. B., and T. D. Tseng, "Gas-Phase Removal of H_2S and NH_3 with Dielectric Barrier Discharges," *J. Environ. Eng., ASCE.*, **122**, 41 (1996).

Chang, M. B., and C. F. Cheng, "Low Temperature SNCR Process for NO_x Control," *Sci. Total Environ.*, **198**, 73 (1997a).

Chang, M. B., and C. F. Cheng, "Plasma-Assisted Removal of NO from Gas Streams via Ammonia Injection," *Environ. Eng. Sci.*, **14**, 193 (1997b).

Chen, L., and W. L. Lee, "Numerical Study for Optimal SNCR Process," *J. Chinese Inst. Environ. Eng.*, **6**, 217 (1996).

Cho, S. M., "Properly Apply Selective Catalytic Reduction for NO_x Removal," *Chem. Eng. Prog.*, **90**, 39 (1994).

Clesceri, L. S., A. E. Greenberg, and R. R. Trussell, *Standard Methods for the Examination of Water and Wastewater*, 17th ed., Chap. 4, APHA-AWWA-WPCE; Washington, D. C., pp. 20 and 111 (1989).

Kline, L. E., W. D. Partlow, and W. E. Bies, "Electron and Chemical Kinetics in Methane rf Glow-Discharge Deposition Plasmas," *J. Appl. Phys.*, **65**, 70 (1989).

Miller, J. A., and C. T. Bowman, ''Mechanism and Modeling of Nitrogen Chemistry in Combustion,'' *Prog. Energy Combust. Sci*., **15**, 287 (1989).

Mizuno, A., K. Shimizu, and A. Chakrabarti, ''NO_x Removal Process Using Pulsed Discharge Plasma,'' *IEEE Trans. Ind. Appl*., **31**, 957 (1995).

Smyth, K. C., ''NO Production and Destruction in a Methane/Air Diffusion Flame,'' *Combust. Sci. Tech*., **115**, 151 (1996).

Sun, W., B. Pashaie, S. K. Dhali, and F. I. Honea, ''Non-Thermal Plasma Remediation of SO_2/NO Using a Dielectric-Barrier Discharge,'' *J. Appl. Phys*., **79**, 3438 (1996).

Thorne, L. R., M. C. Branch, D. W. Chandler, R. J. Kee, and J. A. Miller, *Proc. Symp. (Int.) Combust*., The Combustion Institute, Pittsburgh, p. 956 (1986).

Van Veldhuizen, E. M., W. R. Rutgers, and V. A. Bityurin, ''Energy Efficiency of NO Removal by Pulsed Corona Discharges,'' *Plasmas Chem. Plasmas Process*, **16**, 227 (1996).

Volponi, J. V., and M. C. Branch, ''Flame Structure of C_2H_2-O_2-Argon and C_2H_2-NO_2-Argon Laminar Premixed Flames,'' *Proc. Symp. (Int.) Combution*, The Combustion Institute, Pittsburgh, p. 823 (1992).

Manuscript received Dec. 14, 1999, and revision received Sept. 5, 2000.